International Journal of Innovative Technology and Exploring Engineering (IJITEE)
ISSN: 2278-3075 (Online), Volume-8 Issue-12, October 2019

Infrared with Visual Image Fusion Based on Two-Scale Decomposition and Sturdy Guided Filtering Technique

M.Santhalakshmi, S.Sukumaran

Abstract: ***Several Infrared (IR) and Visual (VIS) image fusion techniques have been widely used to acquire a novel image which may characterize the image accurately, completely and reliably. This process can serve an essential part in image processing applications. In this article, an enhanced IR and VIS image fusion technique is proposed by Two-Scale Decomposition (TSD) and Sturdy Guided Filtering (SGF) together to further increase the robustness of fusion process. Initially, IR and VIS images are decomposed for creating the base and detail layers. Then, Phase Congruency (PC) and Sum Modified Laplacian(SML) are applied to get saliency maps of base and detail layers, respectively. Also, Iteratively Reweighted Least Squares (IRLS) algorithm with GF, namely SGF is included instead of GF method in an efficient manner to properly smooth the weighting maps by preserving the depth edges that correspond to weak color edges and small structures. In this SGF technique, Enhanced Preconditioned Conjugate Gradient (EPCG) method is applied to optimize the RLS iteratively and select the conjugate paths for each iteration efficiently. This SGF can achieve high convergence rate and handle the structure inconsistency while properly preserving the edges. Experimental outcomes exhibit that the proposed TSD-PS-SGF based image fusion technique has higher performance over state-of-the-art techniques in terms of image feature-based, information theory-based and image structure-based metrics.***

Index Terms**:** ***Image Fusion, Two-scale Decomposition, Guided filter, Phase Congruency, Sum modified Laplacian, Enhanced Preconditioned Conjugate Gradient***

I. INTRODUCTION

Images captured from multi-modalities such as optical cameras, low-light dark vision cameras, IR cameras may contain complementary details. IR images have some information with high contrast about the captured sight compared to the visual image. In contrast, visual image has a lot of high-frequency details but has a bad target contrast specifically under bad luminance condition.

Revised Manuscript Received on October 30, 2019.
***** Correspondence Author
M.Santhalakshmi*, Ph.D Research Scholar, Department of Computer Science, Erode Arts and Science College, Erode-638 009, Tamilnadu, India.
Dr.S.Sukumaran, Associate Professor in Computer Science, Erode Arts and Science College, Erode-638 009, Tamilnadu, India.

As a result, the low-light VIS and IR image fusion is one of the techniques widely used in the applications of face detection, night vision surveillance, vehicle navigation and forecasting applications. Image fusion can merge significant details from different image sensors and thus image fusion techniques are used to add IR and VIS images into a single fused image. Therefore, a more perfect and absolute portrayal of the sight is achieved.

In recent times, a huge number of IR and VIS image fusion techniques have been projected. In accordance with the different phases of the fusion procedure, these techniques may be categorized into pixel-level fusion, feature-level fusion and decision-level fusion. Among these categories, pixel-level fusion is the most well-known techniques which can preserve significant information from source images [1-3]. The analysis of these techniques shows that it is valuable, however results in a distorted image. As well, multi-scale image fusion techniques include contourlet, wavelet [4-5] and Non-Subsample contourlet transform (NSCT), [6-7] etc., are useful in the area of IR and VIS images fusion, since an individual visualization is influence to the characteristics of different image channels. The main benefit of these techniques is that the fused images can maintain additional information of actual imagery. Nonetheless, intensity and chromaticity distortions may be generated due to missing of spatial consecutiveness. To tackle this issue, a GF-based Fusion (GFF) technique[8-9] was proposed. GF technique can evade the synthetic texture in the filtering and thus it is used for smoothing the weighting map in the fusion process. Though the GFF technique can absolutely develop the spatial stability in the fusion process, however outcomes of the GFF technique may neglect few information since GF tends to smooth the weighting map.

As a result, Wang et al. [10] proposed an alternative image fusion technique by TSD with the characteristics of GF. Initially, IR and VIS images are decomposed with a two-scale median filter for generating the base and detail layers. Then, PC with GF fusion law is adopted to get saliency maps of base layer and the SML with GF fusion rule is adopted to get saliency maps of detail layers. Based on this TSD-PS-GF technique, the artifacts are removed by smoothing the weighting maps. At last, the resulting image is reformed by accumulating the base and detail of source IR and VIS images. Conversely, the edge preservation of both VIS and IR images require additional methods to increase the robust against the heavy noise and structure inconsistency.

Therefore in this article, an enhanced novel IR and VIS image fusion technique, named TSD-PS-SGF is proposed by combining TSD and SGF to further increase the robustness of fusion process. In this technique, SGF is proposed instead of using GF in which IRLS algorithm is used in an efficient manner to properly smooth the weighting maps by preserving the depth edges that correspond to weak color edges and small structure.

Moreover, Enhanced Preconditioned Conjugate Gradient (EPCG) method is proposed that iteratively selects the conjugate paths for each iteration to optimize the RLS efficiently. This SGF can achieve high convergence rate and handle the structure inconsistency while properly preserving the edges.

The rest of the article is organized as follows: Section II presents the literature survey related to the previous two-scale image fusion techniques. Section III describes the proposed TSD-PS-SGF based image fusion technique. Section IV illustrates the performance analysis of the TSD-PS-SGF technique. Finally, Section V concludes the entire discussion.

II. LITERATURE REVIEW

Adu et al. [11] proposed a NSCT for fusing the IR and VIS light images. Initially, NSCT was used to decompose two real images into low-frequency subband coefficients and the band pass direction subband coefficients. Then, the low-frequency subband coefficients and the bandpass direction subband coefficients were chosen by the local optical features and a least local cross-gradient process, respectively. The cross-gradient was achieved by computing the gradient between the pixel of band pass subbands and the neighbouring pixel in the fused image of the low-frequency components. However, it causes brightness and chromaticity distortions since the spatial consecutiveness was not considered.

Bavirisetti & Dhuli [12] proposed a saliency detection and TSD in which a novel weight map was constructed based on visual saliency. This method was able to combine the visually important details of source images into the fused image. Also, two-scale image decomposition was used instead of multi-scale fusion technique. However, their weight map construction process can barely eliminate some other salient regions which have no relation to the IR target.

Mishra et al. [13] proposed TSD and modified Frie-Chen operators for fusing the images acquired from IR and VIS image sensors and its corresponding hardware implementation. In this method, a simple directional operator was used in the feature detection for discovering features such as edges, lines and the diagonal information. Also, First-In-First-Out (FIFO) based processing was used for reducing the memory consumption. However, the performance efficiency was less. Li et al. [14] proposed an efficient technique based on saliency detection and IR target segmentation. Initially, an image descriptor was introduced and the saliency algorithm was implemented for obtaining the IR image region of interest. Then, an IR target was segmented from the region of interest by adopting the thresholding method. As well, the IR target was added to the fused image. However, the sensitivity and specificity of this method were less.

Hu and Shi [15] proposed Non-Subsampled Shearlet Transform (NSST) and Block Compressive-Sensing Sampling (BCSS) technique for fusing IR and VIS images. In this technique, the source images were decomposed by using NSST and then a fusion rule was used based on local-region energy maximum-choosing for low-frequency subbands. Also, a local-region energy based on BCCS was defined while choosing a maximum for the high-frequency subbands. After that, the inverse NSST was applied to get a resultant fused image. However, the computation time was high. Zhang et al. [16] proposed a novel wavelet-based algorithm for fusing the multi-exposed images. This algorithm has three phases such as changing the input images into YUV space and combining the color-difference components U and V in accordance with the dispersion weight, changing Y into the wavelet domain and combining the corresponding near sub-bands and detail sub-bands by the well-exposedness weight and tuned contrast weight, respectively and changing the fused image into RGB space for obtaining the absolute outcome. However, the computation time was high.

Du et al. [17] proposed a novel method for fusing IR and VIS images of different resolutions and generating high-resolution images to acquire understandable and perfect fused images. In this method, the fusion difficulty was devised as a Total Variation (TV) minimization problem. The data reliability term limits the pixel intensity resemblance of the down sampled fused image with respect to the IR image and the regularization term induces the gradient resemblance of the fused image with respect to the VIS image. As well, the Fast Iterative Shrinkage-Thresholding Algorithm (FISTA) was applied for improving the convergence rate. However, the staircase effects were produced by this method.

III. PROPOSED METHODOLOGY

In this section, the proposed TSD-PS-SGF based fusion technique is explained in brief. The proposed technique has four phases such as TSD, generation of saliency of base and detail layers with PC and SML, respectively, computing weighting maps with SGF and two-scale image restoration. The schematic visualization of the TSD-PS-SGF technique is shown in Figure 1.

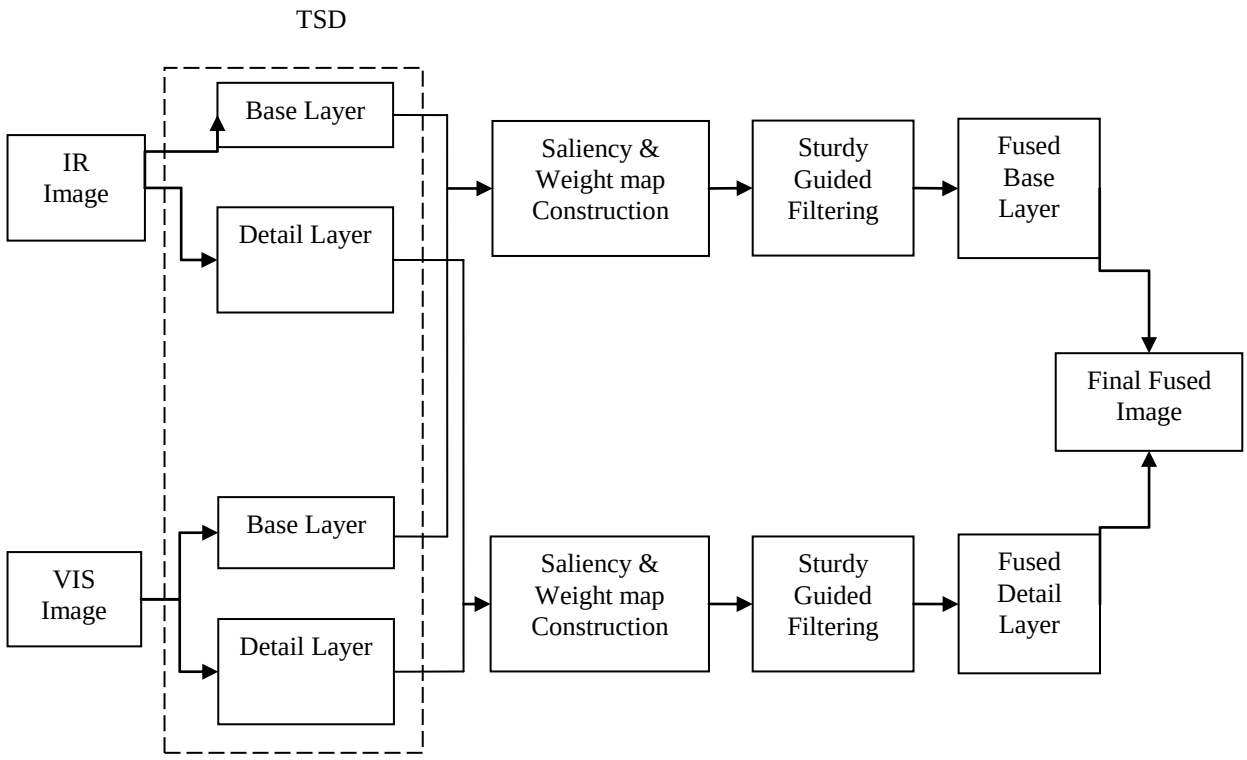

Figure.1 Schematic Visualization of TSD-PS-SGF Technique

3.1 TSD and Saliency Map Generation

Initially, the source images $I_n(i,j)$ are decomposed by TSD method in which a median filter is used to approximate the base layer as:

$$X_n(i,j) = I_n(i,j) * \mu(i,j) \quad (1)$$

In Eq. (1), n represents the n^{th} source image and μ denotes the median filter. The range of median filter is set to 35×35 to obtain the detail layer as:

$$Y_n(i,j) = I_n(i,j) - X_n(i,j) \quad (2)$$

Then, PC technique is adopted to create saliency maps of base layer. The PC is computed by extracting the phase details using log-Gabor filter as:

$$PC(i) = \frac{\sum_l E_l(i)}{\sum_l \sum_n A_{nl}(i) + \varepsilon} \quad (3)$$

In Eq. (3), l is the orientation, $A_{nl}(i)$ denotes the sum of amplitudes, $E_l(i)$ denotes the local energy and ε refers to the small constant coefficient for preventing the zero denominator, so:

$$E_l(i) = \sqrt{F(i)^2 + H(i)^2} \quad (4)$$

$$F(i) = \sum_n s_{nl}(i), H(i) = \sum_l h_{nl}(i) \quad (5)$$

$$A_{nl}(i) = \sum_l \sqrt{s_{nl}(i)^2 + h_{nl}(i)^2} \quad (6)$$

In Eq. (6), $s_{nl}(i)$ and $h_{nl}(i)$ are outcome of the even symmetric and odd filters, correspondingly. After that, the saliency map of base layer is determined via:

$$S_l^b(i,j) = P\left(b_l(i,j)\right) \quad (7)$$

In Eq. (7), S_l^b estimates the saliency map of n^{th} base layer and $P(\cdot)$ is the PS operator. A large SML is used to create the saliency maps of detail layer. Consider the location of pixel is a, thus SML at pixel a is described like:

$$SML(a) = \sum_{k=\omega_a} ML(k)^2 \quad (8)$$

In this algorithm, the pixel a is used as the centroid to construct a rectangular window ω_a. If $k = (i,j)$, then

.

$$ML(i,j) = |2d_l(i,j) - d_l(i-step,j) - d_l(i+step,j)| + |2d_l(i,j) - d_l(i,j-step) - d_l(i,j+step)| \quad (9)$$

In Eq. (9), d_l is the n^{th} detail layer and $step$ is the distance between pixels.

3.2 Weighted Map Construction

At first, the weighted maps are generated by evaluating the saliency maps. After that, the GF is applied to enhance the spatial stability of weighted maps in which the parameters are optimized based on the IECGRLS algorithm. The weighted maps of detail layers in VIS and IR images are P_{VIS}^d and P_{IR}^d determined by comparing the saliency maps of this layer as:

$$P_{VIS}^d = \begin{cases} 1, & S_{VIS}^d > S_{IR}^d \\ 0, & Otherwise \end{cases}; \; P_{IR}^d = 1 - P_{VIS}^d \quad (10)$$

Similarly, the weighted maps of base layers in VIS and IR images are also computed as:

$$P_{VIS}^b = \begin{cases} 1, & S_{VIS}^b > S_{IR}^b \\ 0, & Otherwise \end{cases}; \; P_{IR}^b = 1 - P_{VIS}^b \quad (11)$$

Normally, the weighted maps are not properly associated with object margins which may generate artifacts in the fused image. Hence, SGF is carried out on each weight map $P_{VIS}^d, P_{VIS}^b, P_{IR}^b$ and P_{IR}^d with equivalent source image $I_n(i,j)$. Therefore, the resultant weighted maps of base and detail layers of both VIS and IR images are as:

$$W_{VIS}^b = G(P_{VIS}^b, X_{VIS}, r_1, \varepsilon_1), W_{IR}^b = G(P_{IR}^b, X_{IR}, r_1, \varepsilon_1) \quad (12)$$

$$W_{VIS}^d = G(P_{VIS}^d, Y_{VIS}, r_2, \varepsilon_2), W_{IR}^d = G(P_{IR}^d, Y_{IR}, r_2, \varepsilon_2) \quad (13)$$

To simplify this SGF filter, the above Eq. (12) & (13) can be rewritten as follows:

$$W_n = G(P, I, r, \varepsilon) \quad (14)$$

Where r and ε are the factors which choose the filter range and blur level of the SGF. Also, P and I are input and guidance image, respectively. This SGF considers that the filtering output P^* of the guidance image I and this is formulated as:

$$P^* = \text{argmin}_{P'}\{(1-\alpha)E_1(P', P) + \alpha E_2(P')\} \quad (15)$$

In Eq. (15), $E_1(P', P)$ denotes the data term that makes the outcome to be consistent with the input target image and $E_2(P')$ denotes the smoothness term that reflects prior knowledge of the smoothness of the solution for construing the weighted maps. The relative significance of these two terms is balanced with the parameter α. The output of this filtering is denoted as P^*. The data term $E_1(P', P)$ should be robust against the artifacts and is defined as follows:

$$E_1(P', P) = \sum_{i\in\Omega}\sum_{j\in N(i)} \omega_{i,j}\varphi\left(\left|P_i' - P_j\right|^2\right) \quad (16)$$

In Eq. (16), Ω is all the coordinates of the target image and $N(i)$ denotes the neighborhood of pixel i which is a $(2r+1)\times(2r+1)$ square patch centered at i. The Gaussian window $\omega_{i,j}$ reduces the weights while j is far from i:

$$\omega_{i,j} = e^{\left(-\frac{|i-j|^2}{2\sigma^2}\right)} \quad (17)$$

In Eq. (17), σ denotes a parameter defined by the user and $\varphi(\cdot)$ is the robust error norm function which is denoted as exponential error norm to model the data term as:

$$\varphi(k^2) = 2\lambda^2\left(1 - e^{\left(-\frac{k^2}{2\lambda^2}\right)}\right) \quad (18)$$

In Eq. (18), λ denotes a user defined constant. Similarly, the smoothness term $E_2(P')$ must be robust against the structure inconsistency between the guidance image and the target image. This is defined as:

$$E_2(P') = \sum_{i\in\Omega}\sum_{j\in N(i)} \omega_{i,j}^g\varphi\left(\left|P_i' - P_j'\right|^2\right) \quad (19)$$

In Eq. (19), $\omega_{i,j}^g$ is the guidance weight computed as follows:

$$\omega_{i,j}^g = e^{\left(-\frac{|i-j|^2}{2\sigma^2}\right)} \cdot e^{\left(-\frac{\sum_{c\in C}\left|I_i^c - I_j^c\right|^2}{|C|\times 2\sigma^2}\right)} \quad (20)$$

In Eq. (20), C denotes different channels of I which can be multiple channels or single channel depending on the application and $|C|$ is the number of channels in C. Also, the function in Eq. (16) is employed to model the smoothness term. Both the guidance weight and the exponential error norm function in the smoothness term make use of the property of both the guidance image and the target image to handle the structure inconsistency. For continuous system, this proposed model is formulated as follows:

$$\frac{\partial E}{\partial P_i'} = (1-\alpha)\sum_{j\in N(i)}\omega_{i,j}d_{i,j}\left(P_i' - P_j\right) + 2\alpha\sum_{j\in N(i)}\omega_{i,j}^g s_{i,j}\left(P_i' - P_j'\right) = 0, i\in\Omega \quad (21)$$

Where

$$d_{i,j} = \varphi'\left(\left|P_i' - P_j\right|^2\right), s_{i,j} = \varphi'\left(\left|P_i' - P_j'\right|^2\right), \varphi'(k^2) = e^{\left(-\frac{k^2}{2\lambda^2}\right)} \quad (22)$$

Here, $\varphi'(k^2)$ is the derivative of $\varphi(k^2)$ defined in Eq. (18). A closed-form solution to Eq. (21) is not obtainable. This solution is solved by iteratively. If $s_{i,j}$ and $d_{i,j}$ are maintained as constant in each iteration where $d_{i,j}^n = \varphi'\left(\left|P_i'^n - P_j\right|^2\right), s_{i,j}^n = \varphi'\left(\left|P_i'^n - P_j'^n\right|^2\right)$ for iteration $n+1$, then Eq. (21) becomes the standard form of the following RLS optimization model as:

$$P'^{n+1} = \text{argmin}_{P'}\{(1-\alpha)\sum_{j\in N(i)}\omega_{i,j}d_{i,j}^n\left(P_i' - P_j\right) + \alpha\sum_{j\in N(i)}\omega_{i,j}^g s_{i,j}^n\left(P_i' - P_j'\right)\} \quad (23)$$

After that, the above Eq. (23) is iteratively solved until the final output satisfies the convergence condition. As Eq. (23) is quadratic in each iteration, it can be minimized by solving the set of linear equations:

$$[(1-\alpha)\sum_{j\in N(i)}\omega_{i,j}d_{i,j}^n + 2\alpha\sum_{j\in N(i)}\omega_{i,j}^c s_{i,j}^n]P_i' - 2\alpha\sum_{j\in N(i)}\omega_{i,j}^g s_{i,j}^n P_j' = (1-\alpha)\sum_{j\in N(i)}\omega_{i,j}d_{i,j}^n P_j \quad (24)$$

This can be rewritten in matrix notation as follows:

$$[(1-\alpha)W^n - 2\alpha S^n]P' = (1-\alpha)Z^n P$$
$$\Rightarrow P'^{n+1} = (1-\alpha)[(1-\alpha)W^n - 2\alpha S^n]^{-1}Z^n P \quad (25)$$

Where P' and P are the vector form of the fused image and the input target image, respectively, W^n denotes a diagonal matrix with $W_{i,j}^n = \sum_{j\in N(i)}\omega_{i,j}d_{i,j}^n + \frac{2\alpha}{1-\alpha}\sum_{j\in N(i)}\omega_{i,j}^g s_{i,j}^n$, S^n denotes the similarity matrix whose elements are $S_{i,j}^n = \omega_{i,j}^g s_{i,j}^n$ and Z^n denotes the other similarity matrix with $Z_{i,j}^n = \omega_{i,j}d_{i,j}^n$. To solve Eq. (25), EPCG method is used which achieves better results and convergence property. The EPCG method is an iterative method whose aim is to minimize the quadratic cost function defined in Eq. (25).The gradient of the quadratic cost function is defined as follows:

$$\nabla P' = (1-\alpha)[(1-\alpha)W - \alpha S]ZP \quad (26)$$

By initializing the iteration, the first residual value is computed as:

$$\bar{r}(1) = -\overline{P'_1} = (1-\alpha)[\alpha S - (1-\alpha)W]ZP \quad (27)$$

The new conjugate direction vector $\bar{D}$ is defined to iterate towards the optimum weighted maps as:

$$\bar{D}(1) = P^T\bar{r}(1) \quad (28)$$

The general weighting map update function is given by:

$$P'^{n+1} = P'^n + \mu_{EPCG}(n)\bar{D}(n) \quad (29)$$

In Eq. (29), $\mu_{EPCG}(n)$ denotes the step-size of EPCG and is given by:

$$\mu_{EPCG}(n) = \frac{r^T(n)PP^Tr(n)}{\bar{D}^TP^TP\bar{D}(n)} \quad (30)$$

The residual vector update is given by:

$$\bar{r}(n+1) = \bar{r}(n) + \mu_{EPCG}(n)P\bar{D}(n) \quad (31)$$

The conjugate direction vector update is given by:

$$\bar{D}(n+1) = P^T\bar{r}(n+1) - \rho(n)\bar{D}(n) \quad (32)$$

A linear search is used for computing $\rho(n)$ which reduces P' as:

$$\rho(n) = \frac{r^T(n+1)PP^Tr(n+1)}{r^T(n+1)PP^Tr(n)} \quad (33)$$

Therefore, the EPCG is used for determining the residual and the corresponding weighting maps until the convergence is satisfied.

3.3 Fused Image Restoration

Two-scale image restoration is achieved by 2 steps. Initially, the fused base layers $\bar{X}$ can be obtained by the following formula:

$$\bar{X} = W_{VIS}^b * X_{VIS} + W_{IR}^b * X_{IR} \quad (34)$$

Similarly, the fused detail layer $\bar{Y}$ is obtained as:

$$\bar{Y} = W_{VIS}^d * Y_{VIS} + W_{IR}^d * Y_{IR} \quad (35)$$

After that, the fused image F is synthesized with the fused base and detail layers as:

$$F = \bar{X} + \bar{Y} \quad (36)$$

Thus, the proposed TSD-PS-SGF based fused technique reduces the artifacts and structure inconsistency efficiently.

Input:	*IR image and VIS image*
Output:	*Fused image*
Step 1:	*Decompose the IR and VIS images into base layer & detail layer using Eqs. (1) & (2);*
Step 2:	*Estimate the saliency map & raw weight map* (P) *of both base layer and detail layer using Eqs. (7), (8) & (10), (11);*
Step 3:	*while(traverse all the windows in the images)* *Smooth out the raw weight map via SGF;* *In each window of size* $(2r+1)\times(2r+1)$*, minimize* $E_1(P', P)$*;* *Initialize* α *in Eq. (15),* σ *for* $\omega_{i,j}$ *in Eq. (17) and* $\omega_{i,j}^{g}$ *in Eq. (20); //IRLS-GF* *Iteration* $n = \frac{N}{2} + 1$*; //EPCG;* *Set* $P'(1) = P'\left(\frac{N}{2}\right)$*;* *Define* $\bar{r}(1)$ *using Eq. (27) and* $\bar{D}(1)$ *using Eq. (28);* *Update the weighting map using Eq. (29), residual vector using Eq. (31) and conjugate direction using Eq. (32);*
Step 4:	*while(Eq. (25) does not converge to the fixed point)* *Update image using Eq. (25);* *End while* *End while*
Step 5:	*Average the results in each window to get the smoothed weight maps;*
Step 6:	*Compute the final fused saliency maps using Eqs. (34) and (35);*
Step 7:	*Construct the fused image;*

IV. RESULTS AND DISCUSSION

In this section, the performance of TSD-PS-SGF is analyzed and compared with the existing techniques i.e., TSD-PS-GF [10] and NSCT-PS-GF [11]. The experiment is carried out on a Windows system with an Intel i7 core CPU and 8GB memory with MATLAB implementation. In this experiment, the TNO image fusion dataset [18-19] is used that consists of increased optical (390-700nm), near-IR (700-1000nm) and long-wave IR (8-12µm) dark images of different military and surveillance applications, viewing different objects and targets in different backgrounds. The comparison is made in terms of an information theory-based metric (Mutual Information (MI)), an image feature-based metric $(Q^{AB/F})$ and an image structure-based metric(Q^{SSIM}).

- MI: It is used to measure the sum of source image details conserved in the fused image.
- $Q^{AB/F}$: This metric is used to measure how well the amount of edge details is preserved in the fused images.
- Q^{SSIM} : This metric utilizes Structural Similarity (SSIM) to measure the sum of SSIM transmitted from the source images to the fused images.

High values of these metrics can specify improved quality of the fused images. Figure 2 and Table 1 shows the evaluation of fusion outcomes made by different fusion techniques for input image 1.


IR Image


Visible Image


Base Layer 1


Base Layer 2

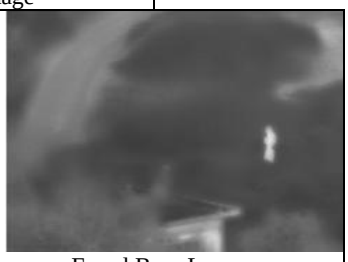
Fused Base Layer

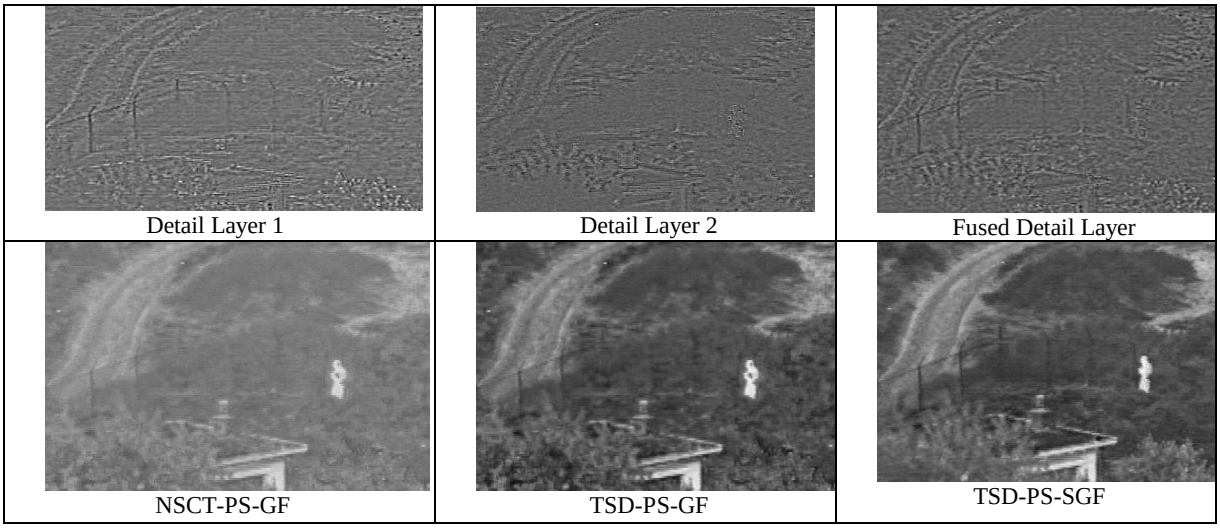

Figure.2 Comparison Outcomes of Fusion Techniques (Image 1)

The quantitative comparisons of the proposed and existing techniques for both input images are given in Table 1.

Table.1 Comparison of Proposed and Existing Techniques

Techniques	MI	$Q^{AB/F}$	Q^{SSIM}
NSCT-PS-GF	2.36	0.544	0.658
TSD-PS-GF	2.43	0.568	0.662
TSD-PS-SGF	2.51	0.592	0.666

Similarly, Figure 3 and Table 2 shows the evaluation of fusion outcomes made by different fusion techniques for input image 2.

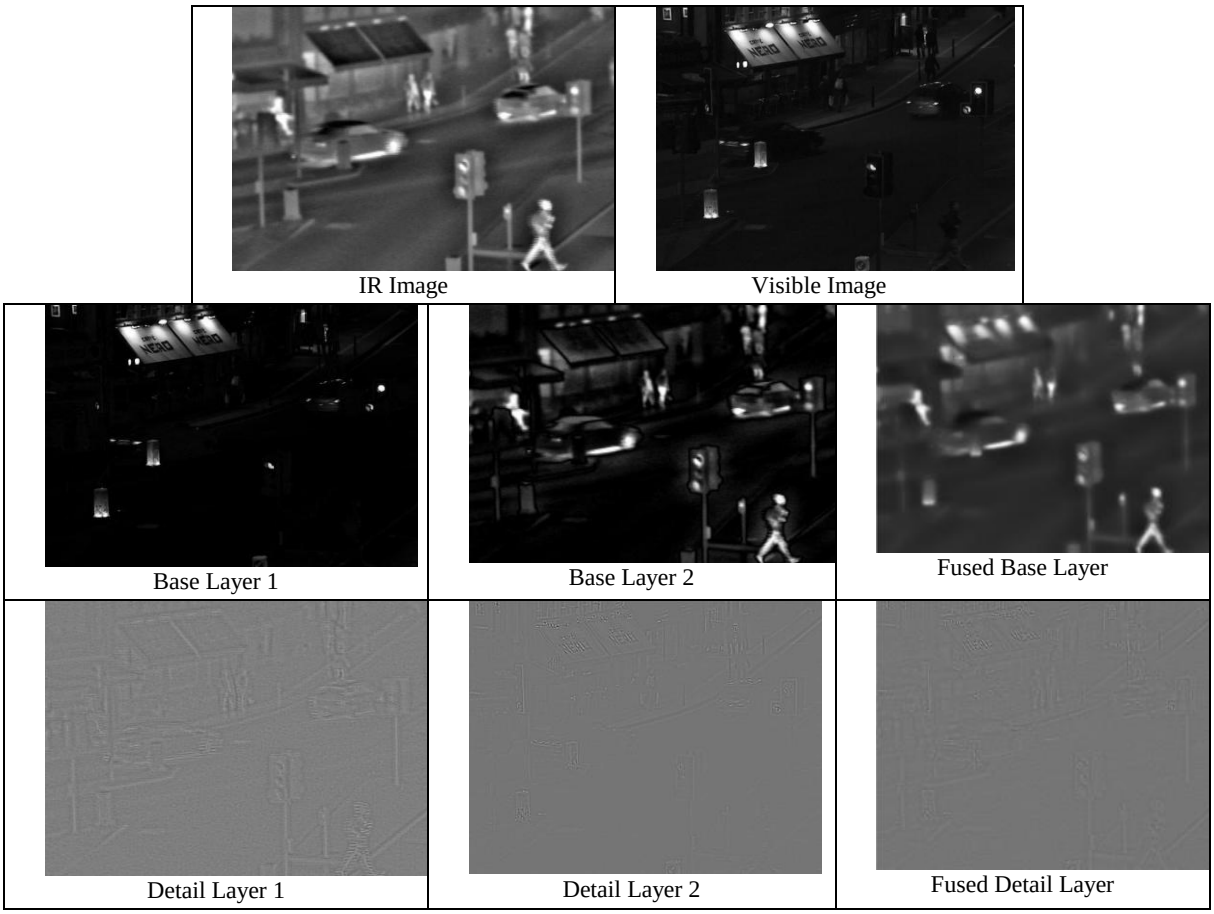

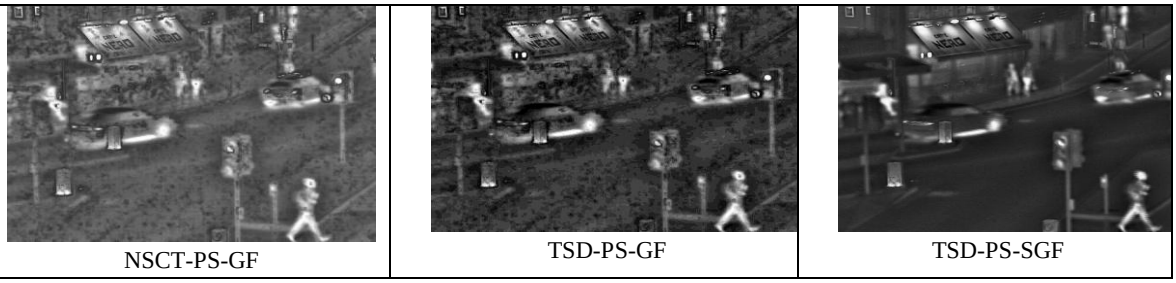

NSCT-PS-GF | TSD-PS-GF | TSD-PS-SGF

Figure.3 Comparison Outcomes of Fusion Techniques (Image 2)

The quantitative comparisons of the proposed and existing techniques for both input images are given in Table 2.

Table.2 Comparison of Proposed and Existing Techniques

Techniques	MI	$Q^{AB/F}$	Q^{SSIM}
NSCT-PS-GF	2.41	0.552	0.665
TSD-PS-GF	2.48	0.559	0.671
TSD-PS-SGF	2.56	0.568	0.677

V. CONCLUSION

In this article, an enhanced novel IR and VIS image fusion technique named TSD-PS-SGF is proposed that combines both TSD and SGF to increase the fusion performance. At first, TSD method is applied to decompose both IR and VIS images that generates the base layers and detail layers. After that, PC and SML are used for obtaining the saliency maps of base and detail layers, correspondingly. Moreover, SGF method is applied based on the IRLS for properly smoothing the weighting maps by preserving the depth edges that correspond to weak color edges and small structures. To optimize the IRLS efficiently, EPCG method is proposed that iteratively chooses the conjugate paths for each iteration. Therefore, the artifacts and structure inconsistency are efficiently prevented by using this technique. Finally, experimental results proved that the proposed TSD-PS-SGF technique has better performance than the existing techniques such as TSD-PS-GF and NSCT-PS-GF in terms of image feature-based, information theory-based and image structure-based metrics.

REFERENCES

1. Suthakar,R.J., Esther, J. M., Annapoorani, D., & Samuel, F. R. S.,"Study of image fusion-techniques, method and applications", International Journal of Computer Science and Mobile Computing, 3(11), 469-476(2014).
2. Pandey, M. (2014). Different Operator Using In Edge Detection For Image Processing. *International Journal Of Computer Science Engineering And Information Technology Research (IJCSEITR)*, *4*(1), 57-62.
3. Sharma, M.,"A review: image fusion techniques and applications", International Journal of Computer Science and Information Technologies, 7(3), 1082-1085 (2016).
4. Thakur,U., Rai, S., & Sahu, S. K.,"A study an image fusion for the pixel level and feature based techniques", Advances in Computational Sciences and Technology, 10(10), 3047-3055(2017).
5. Betigeri, A. S., & Dixit, M. A. N. A. S. I. (2014). Modification In Human Face Image For Personal Identification. *International Journal of Applied Engineering Research and Development*, *4*(2), 13-22.
6. Budhewar, S.T, "Wavelet and curvelet transform based image fusion algorithm", International Journal of Computer Science and Information Technologies, 5(3), 3703-3707(2014).
7. Sundari, P. M., & Kumar, S. B. R. (2014). A study of image processing in analyzing tree ring structure. *Int. J. Res. Humanit. Arts Lit*, *2*(3), 13-18.
8. Panda, B.,"Image fusion using combination of wavelet and curvelet fusion", International Journal of Advanced Research in Computer Engineering & Technology, 5(8), 2316-2324(2016).
9. Xu, L., Du, J., & Li, Q.," Image fusion based on nonsub sampled contourlet transform and saliency-motivated pulse coupled neural networks", Mathematical Problems in Engineering (2013).
10. MUHAMEDIYEVA, D. (2014). Population models with nonlinear diffusion of Kolmogorov-Fisher type. *International Journal in Research in Applied, Natural and Social Science*, *2*(2), 1-10.
11. Liu, Y., Liu, S., & Wang, Z., "Medical image fusion by combining Nonsubsampled contourlet transform and sparse representation", In Chinese Conference on Pattern Recognition (pp.372-381).Springer, Berlin, Heidelberg (2014).
12. Abbas, A. S., Jeberson, W., & Klinsega, V. V. (2013). IMPLEMANTATION OF FUSION MODEL TO RE-ENGINEER LEGACY SOFTWARE. *International Journal of Computer Science and Engineering (IJCSE)*.
13. He, K., Sun, J., & Tang, X.," Guided image filtering", IEEE Transactions on Pattern Analysis And Machine Intelligence, 35(6), 1397-1409(2013).
14. Li, S., Kang, X., & Hu, J., "Image fusion with guided filtering", IEEE Transactions on Image processing, 22(7), 2864-2875(2013).
15. Wang, X., Nie, R., & Guo, X. ,"Two-scale Image Fusion of Visible and Infrared Images Using Guided Filter", In Proceedings of the 7th International Conference on Informatics, Environment, Energy and Applications (pp. 217-221). ACM(2018).
16. Adu, J., Gan, J., Wang, Y., & Huang, J.,"Image fusion based on Nonsubsampled contourlet transform for infrared and visible light image", Infrared Physics & Technology, 61, 94-100(2013).
17. Bavirisetti, D. P., & Dhuli, R.," Two-scale image fusion of visible and infrared images using saliency detection", Infrared Physics & Technology, 76, 52-64(2016).
18. Kamis, A., Mamat, R. O. S. M. A. W. A. T. I., Safie, N. S., & Mustapha, R. A. M. L. E. E. (2015). Spatial visualization ability among apparel design students. *Best: International Journal of Humanities, Arts, Medicine and Sciences*, *3*, 15.
19. Mishra, A., Mahapatra, S., & Banerjee, S.,"Modified Frei-Chen operator-based infrared and visible sensor image fusion for real-time applications", IEEE Sensors Journal, 17(14), 4639-4646(2017).
20. Li, J., Song, M., &Peng, Y.,"Infrared and visible image fusion based on saliency detection and infrared target segment", In 2017 2nd International Conference on Computer Engineering, Information Science and Internet Technology, pp. 21-30 (2017).
21. Hu, D., & Shi, H. ,"Fusion of infrared and visible images based on Nonsubsampled shearlet transform and block compressive sensing sampling", Ukrainians Journal of Physical Optics, 18(3), 156-167(2017).
22. Zhang, W., Liu, X., Wang, W., & Zeng, Y., "Multi-exposure image fusion based on wavelet transform", International Journal of Advanced Robotic Systems, 15(2), 1-19(2018).
23. Du, Q., Xu, H., Ma, Y., Huang, J., & Fan, F.," Fusing infrared and visible images of different resolutions via total variation model", Sensors, 18(11), 3827 (2018).
24. FigShare.Availableonline:https://figshare.com/articles/TNO_Image_Fusion_Dataset/1008029 (accessed on 1 March 2019).
25. Toet, A., The TNO multiband image data collection. Data in Brief, 15, 249-251(2017).

AUTHORS PROFILE

M.Santhalakshmi received the Bachelor of Computer Science (B.Sc.) degree from the Bharathiar University, Coimbatore, TN, India, in 2010 and the Master of Computer Science (M.S.C.) degree from the Bharathiar University, Coimbatore, TN, India, in 2013. She also recieved the M.Phil degree from the Bharathiar University, Coimbatore, in 2014. She is pursuing Ph.D degree in computer science at Bharathiar University. Her research interests include digital image processing.

Dr. S. Sukumaran graduated in 1985 with a degree in Science. He obtained his Master Degree in Science and M.Phil in Computer Science from the Bharathiar University. He received the Ph.D degree in Computer Science from the Bharathiar University. He has 30 years of teaching experience starting from Lecturer to Associate Professor. At present he is working as Associate Professor of Computer Science in Erode Arts and Science College, Erode, Tamilnadu. He has guided for more than 55 M.Phil research Scholars in various fields and guided 13 Ph.D Scholars. Currently he is Guiding 3 M.Phil Scholars and 6 Ph.D Scholars. He is member of Board studies of various Autonomous Colleges and Universities. He published around 80 research papers in national and international journals and conferences. His research interests include Image processing, Network Security and Data Mining.